A Practical Analytic Model for Daylight

A. J. Preetham Peter Shirley Brian Smits

University of Utah www.cs.utah.edu

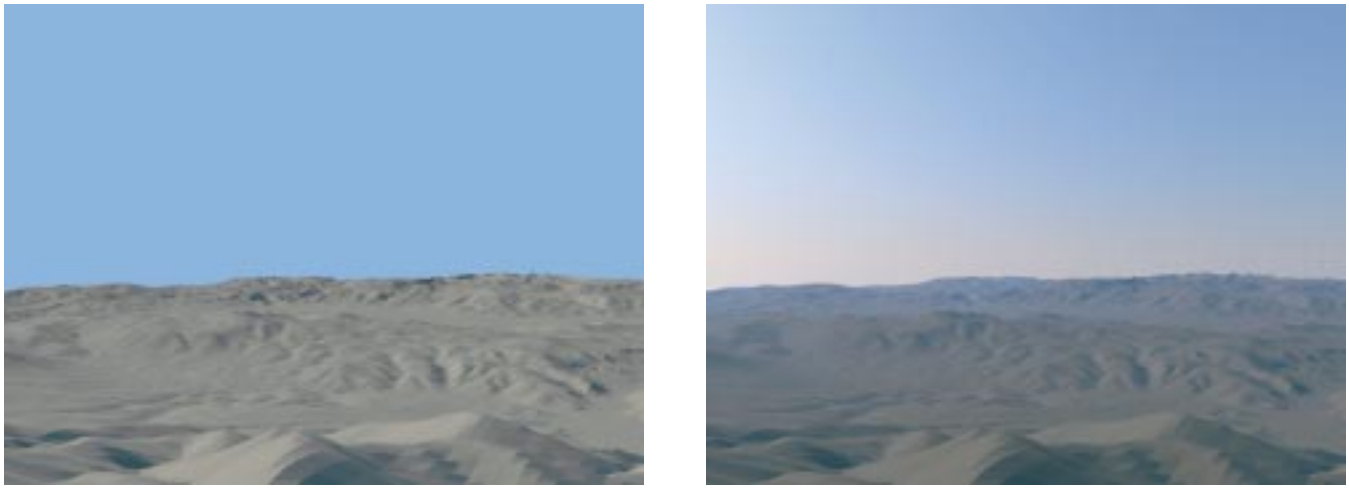

Figure 1: *Left: A rendered image of an outdoor scene with a constant colored sky and no aerial perspective. Right: The same image with a physically-based sky model and physically-based aerial perspective.*

Abstract

Sunlight and skylight are rarely rendered correctly in computer graphics. A major reason for this is high computational expense. Another is that precise atmospheric data is rarely available. We present an inexpensive analytic model that approximates full spectrum daylight for various atmospheric conditions. These conditions are parameterized using terms that users can either measure or estimate. We also present an inexpensive analytic model that approximates the effects of atmosphere (aerial perspective). These models are fielded in a number of conditions and intermediate results verified against standard literature from atmospheric science. These models are analytic in the sense that they are simple formulas based on fits to simulated data; no explicit simulation is required to use them. Our goal is to achieve as much accuracy as possible without sacrificing usability.

CR Categories: I.3.7 [Computing Methodologies]: Computer Graphics—Three-Dimensional Graphics and RealismColor, shading, shadowing, and texture

Keywords: sunlight, skylight, aerial perspective, illumination

1 Introduction

Most realistic rendering research has dealt with indoor scenes. Increased computing power and ubiquitous measured terrain data has made it feasible to create increasingly realistic images of outdoor scenes. However, rendering outdoor scenes is not just a matter of scaling up rendering technology originally developed for indoor scenes. Outdoor scenes differ from indoor scenes in two important aspects other than geometry: most of their illumination comes directly from the sun and sky; and the distances involved make the effects of air visible. These effects are manifested as the desaturation and color shift of distant objects and is usually known as *aerial perspective*. In this paper we present an efficient closed form approximation that captures the visually salient aspects of these phenomena and is easy to incorporate into a rendering system. Our approach is motivated by the desire to generate images of real terrain, so we pay attention to maintaining physically-based radiometry, and use input parameters that are readily available to computer graphics researchers. We feel that current approaches are either far too general and expensive to be easily used, or include too many simplifications to generate a sufficiently realistic appearance.

The importance of the phenomena modeled in this paper is emphasized in the psychology and art literature. Psychologists assert that aerial perspective is a fundamental depth cue that humans use to estimate distances, and the only absolute depth cue available for distant unfamiliar objects [10]. Painters use aerial perspective and variation in sky color in almost all landscape paintings. Da Vinci devoted an entire chapter of his notebooks to the painting of these effects [6]. He stated several characteristics that painters should capture including the whitening of the sky toward the horizon, the increasing density of aerial perspective toward the ground, and the hue shift of distant objects. Any models of the sky and aerial perspective should make sure they capture these subjective effects. The

model presented in this paper does capture these effects and is careful to predict their magnitude and color as well. Rendered images with and without these effects are shown in Figure 1. The image on the right of Figure 1 was rendered using the techniques from this paper.

To produce a realistic outdoor image, we need to model the aspects of atmosphere that produce the color of the sky and the effects of aerial perspective. To be most convenient and efficient for rendering, two formulas are needed. The first should describe the spectral radiance of the sun and sky in a given direction. The second should describe how the spectral radiance of a distant object is changed as it travels through air to the viewer. Although computer graphics researchers have captured these effects by explicit modeling, there has so far been no such compact formulas that do not introduce gross simplifications (e.g., the sky is a uniform color).

While it is possible to directly simulate the appearance of a particular sky given particular detailed conditions, this is inconvenient because it is a complex and CPU-intensive task, and data for detailed conditions is generally not available. It would be more convenient to have a parameterized formula that takes input data that is generally available, or is at least possible to estimate. While such formulas exist for sky luminance, there have not been any for sky spectral radiance. Given a sky spectral radiance formula, there have been no closed-form formulas that account for accurate aerial perspective. This paper presents such a set of formulas that are parameterized by geographic location, time and date, and atmospheric conditions. The formulas are for clear and overcast skies only. While we do not present results for partially cloudy skies, our clear sky results should be useful for developing such a model.

Our formulas are parametric fits to data from simulations of the scattering in the atmosphere. These models are analytic in the sense that they are simple formulas based on fits to simulated data; no explicit simulation is required to use them. We will downplay the mechanics of our simulation which is based largely on previous work in computer graphics. Instead we emphasize a careful discussion on its underlying assumptions and accuracy as well as all material needed to implement our model. In Section 2 we review previous work on modeling the atmospheric phenomena that are responsible for the appearance of the sky and objects under natural illumination. In Section 3 we describe a new model for the spectral radiance of the sun and sky. In Section 4 we extend that model to include the effects of aerial perspective. We present images created using these models in Section 5. We discuss limitations of the models and future work in Section 6. All needed formulas and data for implementing the model are given in the appendices.

2 Background

Many applications use estimates of energy levels of skylight and sunlight to aid in simulation. For this reason modeling skylight has been studied in many fields over several decades. For rendering, we need a function of the form:

$$\textit{sky} : (\text{direction, place, date/time, conditions}) \rightarrow \text{spectral radiance}.$$

Here "place" is the geographic coordinates (e.g., latitude/longitude) of the viewer. Such a formula would allow a renderer to query the sky for a color in a specific direction for either display or illumination computation. The spectral radiance of the sun should in principle be given by a compatible formula.

In this section we review previous approaches to generating formulas related to the sky function above. We will see that no efficient formula of the form of *sky* has previously appeared, but that many techniques are available that bring us close to that result.

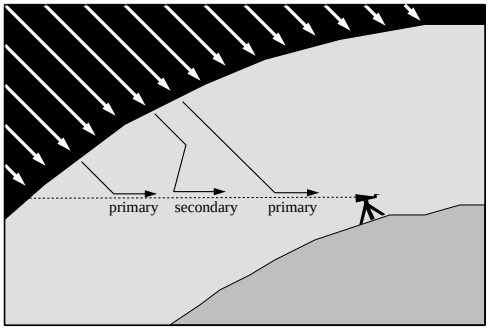

Figure 2: *The earth's atmosphere receives almost parallel illumination from the sun. This light is scattered into the viewing direction so that the sky appears to have an intrinsic color. Light may scatter several times on the way to the viewer, although primary scattering typically dominates.*

2.1 Atmospheric Phenomena

The visually rich appearance of the sky is due to sunlight scattered by a variety of mechanisms (Figure 2). These mechanisms are described in detail in the classic book by Minnaert [22], and with several extensions in the more recent book by Lynch and Livingston [19]. For a clear sky, various types of atmospheric particles are responsible for the scattering. Because the scattering is not necessarily the same for all light wavelengths, the sky takes on varying hues.

The details of the scattering depend on what types of particles are in the atmosphere. Rayleigh developed a theory for scattering by air molecules less than 0.1λ in diameter [28]. The crux of the theory is that the monochromatic optical extinction coefficient varies approximately as λ^{-4}, and this has been verified experimentally. This means that blue light (400nm) is scattered approximately ten times as much as red light (700nm), which is the usual explanation for why the sky is blue. Because the short wavelengths in sunlight are preferentially scattered by the same effect, sunlight tends to become yellow or orange, especially when low in the sky because more atmosphere is traversed by the sunlight on the way to the viewer.

Although Rayleigh scattering does explain much of the sky's appearance, scattering from haze is also important. The term *haze* refers to an atmosphere that scatters more than molecules alone, but less than fog [21]. Haze is often referred to as a *haze aerosol* because the extra scattering is due to particles suspended in the molecular gas. These particles are typically much bigger than molecules, and Mie scattering models the scattering behavior of these particles. Because the haze particles typically scatter more uniformly than molecules for all wavelengths, haze causes a whitening of the sky. The actual particles come from many sources – volcanic eruptions, forest fires, cosmic bombardment, the oceans – and it is very difficult to precisely characterize the haze of a given sky. Many researchers, starting with Angstrom, have attempted to describe haze using a single heuristic parameter. In the atmospheric sciences literature, the parameter *turbidity* is used [21].

Turbidity is a measure of the fraction of scattering due to haze as opposed to molecules. This is a convenient quantity because it can be estimated based on visibility of distant objects. More formally, turbidity T is the ratio of the optical thickness of the haze atmosphere (haze particles and molecules) to the optical thickness of the atmosphere with molecules alone:

$$T = (t_m + t_h)/t_m,$$

where t_m is the vertical optical thickness of the molecular atmosphere, and t_h is the vertical optical thickness of the haze atmosphere. Optical thickness for a given path is given by $\int_0^s \beta(x)dx$

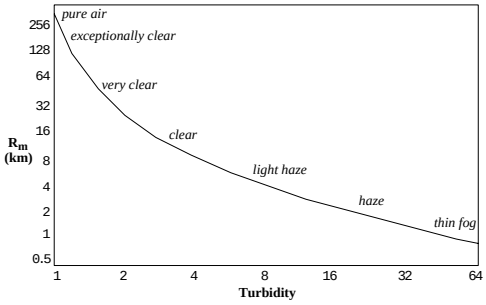

Figure 3: *Meteorological range R_m for various turbidity values. Values computed from source data in McCartney [21]*

where $\beta(x)$ is the scattering coefficient (fraction scattered per meter of length traveled) which may vary along the path. Several other definitions of turbidity are used in various fields, so some care must be taken when using reported turbidity values. Since turbidity varies with wavelength, its value at 550nm is used for optical applications [21]. Turbidity can also be estimated using meteorologic range, as is shown in Figure 3. Meteorological range R_m is the distance under daylight conditions at which the apparent contrast between a black target and its background (horizon sky) becomes equal to the threshold contrast ($\epsilon = 0.02$) of an observer, and it roughly corresponds to the distance to most distant discernible geographic feature.

Although turbidity is a great simplification of the true nature of the atmosphere, atmospheric scientists have found it a practical measure of great utility. Because it does not require complex instrumentation to estimate turbidity, it is particularly well-suited for application in graphics, and we use it to characterize atmospheric conditions throughout the rest of this paper.

2.2 Atmospheric Measurements and Simulation

One way to develop a sky model is to use measured or simulated data directly. The CIE organized the International Daylight Measurement Program (IDMP) to collect worldwide information on daylight availability. Several other efforts have collected measured data that can be used directly. The data sources do not include spectral radiance measurements, so they are not directly useful for our purposes. Ineichen et al. surveyed these data sources and compared them to analytic sky luminance models [12]. They did find that existing sky luminance models are reasonably predictive for real skies in a variety of locations around the world.

Various computer graphics researchers have simulated atmospheric effects. Blinn simulated scattering for clouds and dusty surfaces to generate their appearance [1]. Klassen used a planar layer atmospheric model and single scattering to simulate sky color [18]. Kaneda et al. employed a similar simulation using a spherical atmosphere with air density changing exponentially with altitude [15]. Nishita et al. extended this to multiple scattering to display sky color [25] and also simulated atmospheric scattering to display earth and atmosphere from space [26]. All of these methods require a lengthy simulation for a given sky condition, but they have the advantage of working with arbitrarily complex atmospheric conditions.

2.3 Analytic Sky Models

For simpler sky conditions, various researchers have proposed parametric models for the sky. Pokrowski proposed a formula for sky luminance (no wavelength information) based on theory and sky measurements. Kittler improved this luminance formula which was later adopted as a standard by the CIE [4]:

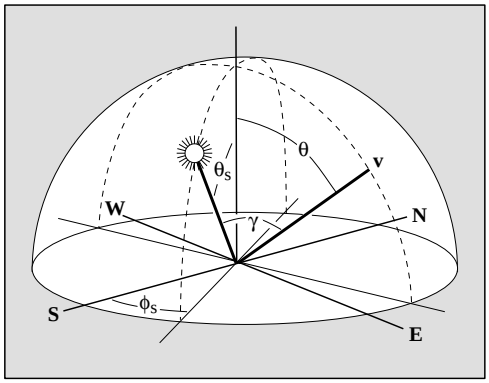

Figure 4: *The coordinates for specifying the sun position and the direction* $\mathbf{v}$ *on the sky dome.*

$$Y_z \frac{\left(0.91 + 10e^{-3\gamma} + 0.45\cos^2\gamma\right)\left(1 - e^{-0.32/\cos\theta}\right)}{\left(0.91 + 10e^{-3\theta_s} + 0.45\cos^2\theta_s\right)\left(1 - e^{-0.32}\right)}, \quad (1)$$

where Y_z is the luminance at the zenith, and the geometric terms are defined in Figure 4. The zenith luminance Y_z can be found in tables [17], or can be based on formulas parameterized by sun position and turbidity [4, 16].

In computer graphics, the CIE luminance formula has been used by several researchers (e.g., [23, 30]). To get spectral data for values returned by the CIE luminance formula, Takagi et al. inferred associated color temperature with luminance levels using empirical data for Japanese skies, and used this color temperature to generate a standard daylight spectrum [29]. In the *Radiance* system the luminance is multiplied by a unit luminance spectral curve that is approximately the average sky color [31].

Moon and Spencer developed a formula for the luminance distribution of overcast skies which was later adopted by the CIE [4]:

$$Y_z\left(1 + 2\cos\theta\right)/3, \quad (2)$$

There are various more complicated formulas for overcast sky luminance, but they vary only subtly from Equation 2 [17]. The zenith values for luminance of overcast skies can be found from tables [17] or from analytic results adopted by CIE [4].

To gain efficiency over brute-force simulations, while retaining the efficiency of the CIE representation, researchers have used basis functions on the hemisphere to fit simulation data. Dobashi et al. used a series of Legendre basis functions for specific sky data [7]. These basis functions can be used to fit any sky data, and does not supply a specific analytic sky model. Rather, it provides a representation and a fitting methodology for some arbitrary data set. These basis functions have the advantage of being orthogonal, but have the associated property that care must be taken to keep the approximation nonnegative everywhere. Because these basis functions are not tailored specifically for sky distributions, many terms might be needed in practice. Our work differs from that of Dobashi et al. in the choice of basis functions. More importantly, we supply the parameters resulting from our simulations, so the formulas in this paper can be used directly.

Nimeroff et al. used steerable basis functions to fit various sky luminance models including the CIE clear sky model [24]. They demonstrated that the steerable property yielded great advantage in rendering applications. They used approximately ten basis functions for their examples.

Brunger used the SKYSCAN data to devise a sky radiance model [2]. His model represented the sky radiance distribution as a

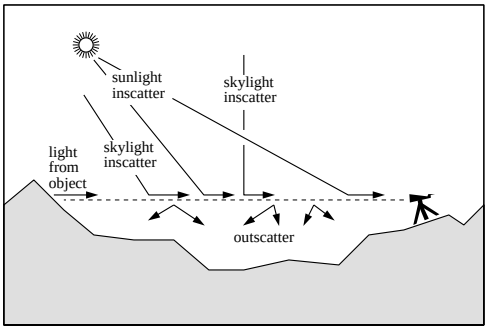

Figure 5: *The color of a distant object changes as the viewer moves away from the object. Some light is removed by out-scattering, and some is added by in-scattering.*

composition of two components, one depending on viewing angle from zenith and the other on scattering angle. An analytic radiance model is very useful for illumination engineers for energy calculations, but what the graphics community needs is a spectral radiance model and not a radiance model.

Perez et al. developed a five parameter model to describe the sky luminance distribution [27]. Each parameter has a specific physical effect on the sky distribution. The parameters relate to (a) darkening or brightening of the horizon, (b) luminance gradient near the horizon, (c) relative intensity of the circumsolar region, (d) width of the circumsolar region and (e) relative backscattered light. These basis functions can be fit to any data, and are designed to capture the overall features of sky distributions without ringing or a data explosion. Perez et al.'s model is given by:

$$\mathcal{F}(\theta,\gamma) = (1 + Ae^{B/\cos\theta})(1 + Ce^{D\gamma} + E\cos^2\gamma), \qquad (3)$$

where A, B, C, D and E are the distribution coefficients and γ and θ are the angles shown in Figure 4. The luminance Y for sky in any viewing direction depends on the distribution function and the zenith luminance and is given by

$$Y = Y_z \mathcal{F}(\theta,\gamma)/\mathcal{F}(0,\theta_s). \qquad (4)$$

The Perez model is similar to the CIE model, but has been found to be slightly more accurate if the parameters A through E are chosen wisely [12]. The Perez formula has been used in graphics with slight modification by Yu et al. [33].

What would be most convenient for computer graphics applications is a spectral radiance analog of Equation 1 that captures the hue variations suggested by real skies and full simulations. Such a form will be introduced in Section 3.

2.4 Aerial Perspective

A sky model is useful for both direct display and illuminating the ground. However, it is not directly applicable to how the atmosphere changes the appearance of distant objects (Figure 5). Unlike a sky model, aerial perspective effects cannot be stored in a simple function or precomputed table because they vary with distance and orientation. A subtlety of aerial perspective is that it can cause color shifts in any direction. Typically, it causes a blue-shift, but when the viewing direction is near the sun, it can cause a yellow-shift. It is hard to predict such color shifts without a physically-based model.

Max presented an analytic single scattering model for light scattering through haze with uniform density and a generalized result for the case of layered fog [20]. Kaneda et al. presented analytical results for fog effects where density variation of fog was exponential [15] which is a special case of Max's layered fog model. However, it is not possible to analytically solve for the extended case of air combined with haze.

Several researchers have simulated aerial perspective using explicit modeling [15, 18]. This in fact is just a particular instance of general light scattering simulation. While such techniques have the advantage of working on arbitrary atmospheric conditions, they are also computationally expensive.

Ward-Larson has implemented a simpler version of aerial perspective in the *Radiance* system [30]. He assumes a constant ambient illumination that does not vary with viewing direction. This produces an efficient global approximation to aerial perspective, but does not allow the changes in intensity and hue effects for changing viewer or sun position.

In Ebert et al., the aerial perspective effect is modeled through a simulation of single Rayleigh scattering [8]. The color of distant mountains is a linear combination of the mountain color and sky color whose weighting varies with distance. They include a sophisticated discussion of how to numerically integrate the resulting expressions. Although they restrict themselves to pure air (turbidity 1), their techniques could easily be extended to include haze because they use numeric techniques. The only shortcoming of their method is that the quadrature they perform is intrinsically costly, although they minimize that cost as much as possible.

3 Sunlight and Skylight

This section describes our formulas for the spectral radiance of the sun and the sky. The input to the formulas is *sun position* and *turbidity*. Sun position can be computed from latitude, longitude, time, and date using formulas given in the Appendix. We assume the *U.S. Standard Atmosphere* for our simulations. We use Elterman's data for the density profile for haze up to 32km [9].

3.1 Sunlight

For sunlight we use the sun's spectral radiance outside the earth's atmosphere, which is given in the Appendix. To determine how much light reaches the earth's surface we need to compute the fraction removed by scattering and absorption in the atmosphere. Sunlight is scattered by molecular and dust particles and absorbed by ozone, mixed gases and water vapor. In what order, this attenuation takes place does not matter because attenuation is multiplicative and thus commutative. Iqbal gives direct radiation attenuation coefficients for the various atmospheric constituents [13], so we can compute the total attenuation coefficient if we know the accumulated densities along the illumination path.

The sun's extraterrestrial spectral radiance is multiplied with the spectral attenuation due to each atmospheric constituents to give us the sun's spectral radiance at earth's surface. Transmissivity due to these constituents are given in the Appendix. To test our formulas we compared the sunlight results at turbidity two with measured values of sun chromaticity and luminance given by Wyszecki and Stiles [32]. These numbers were with two percent of each other.

3.2 Skylight Model

Skylight is much more complicated to model than sunlight. Given a model for the composition of the atmosphere, we can run a simulation using the methods of previous researchers. However, we would then have the data for only one turbidity and sun position. What we do is compute the sky spectral radiance function for a variety of sun positions and turbidities, and then fit a parametric function. Basic issues that must be addressed are the assumptions used for the simulation, and the parametric representation we use to fit the data.

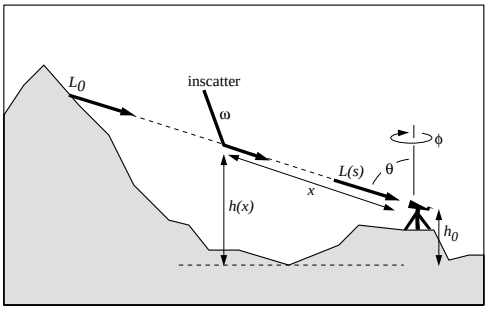

Figure 6: *The variables used to compute aerial perspective.*

For the simulation we used the method of Nishita et al. [25]. The earth was assumed flat for zenith angles less than seventy degrees and spherical for other angles. This allowed several terms to be evaluated analytically for the smaller angles. Third and higher order scattering terms were ignored as their contribution to skylight is not significant. Reflectance of light from the earth's surface was also ignored. This simulation was run for twelve sun positions and five different turbidities (2 through 6). The spectral radiance was computed for 343 directions in a sky dome for each of these combinations. Because the amount of computation required was large (about 600 CPU hours in all) a number of careful optimizations were employed to make the computation feasible such as an aggressive use of lookup tables and adaptive sampling of directions.

For our parametric formula for luminance we use Perez et al.'s formulation (Equation 4). This formulation has been battle-tested and has few enough variable that the optimization stage of the fitting process is likely to converge. We use this in preference to the CIE model because it has a slightly more general form and can thus capture more features of the simulated data. To account for spectral variation, we also fit chromatic variables. We found Perez's formulation to be a poor way to represent the CIE X and Z variables, but the chromaticities x and y are well represented with this five parameter model. The functions were fit using *Levenberg-Marquardt* non-linear least squares method in MATLab [11]. A linear function in turbidity was obtained to describe the five parameters for Y, x and y. The zenith values for Y, x and y were also fit across different sun positions and turbidities.

Chromaticity values x and y are similarly behaved and are given by the same model. Thus,

$$x = x_z \frac{\mathcal{F}(\theta,\gamma)}{\mathcal{F}(0,\theta_s)}, \text{ and } y = y_z \frac{\mathcal{F}(\theta,\gamma)}{\mathcal{F}(0,\theta_s)},$$

where $\mathcal{F}$ is given by Equation 3 with different values of (A,B,C,D,E) for x and y. The distribution coefficients and zenith values for luminance Y, and chromaticities x and y are given in the Appendix. The luminance Y and chromaticities x and y can be converted to spectral radiance on the fly using the CIE daylight curve method described in the Appendix.

4 Aerial Perspective Model

Unlike the sun and sky, aerial perspective cannot be precomputed for a given rendering. At every pixel it is a complex integral that must be evaluated numerically. Because we want to capture the subjective hue and intensity effects of aerial perspective we must preserve a reasonable degree of accuracy. But to make the problem tractable we assume a slightly simpler atmospheric model than we did for skylight: we approximate the density of the particles as exponential with respect to height. The rate of decrease is different for the two gas constituents. This does not make the aerial perspective equations solvable analytically, but it does make them tractable enough to be approximated accurately. This approximation will be described for the rest of this section. We assume that the earth is flat, which is a reasonable assumption for viewers on the ground.

Aerial perspective results when the light L_0 from a distant object is attenuated on the way to the viewer. In addition, light from the sun and sky can be scattered towards the viewer. This is shown in Figure 6. If τ is the extinction factor as L_0 travels a distance s to reach the eye, and L_{in} is the in-scattered light, then $L(s) = L_0\tau + L_{in}$.

Both the extinction factor τ and the in-scattered light L_{in} are a result of the scattering properties of the different particles in the atmosphere. Because the scattering coefficients of particles is proportional to the density of particles, the scattering coefficients also decrease exponentially with height. Thus, $\beta(h) = \beta^0 e^{-\alpha h}$, where β^0 is the value of scattering coefficient at earth's surface and α is the exponential decay constant. In our case, h is a function of the distance from the viewer, as shown in Figure 6, and can be represented as $h(x) = h_0 + x\cos\theta$. We can now write the expression for β as

$$\beta(h(x)) = \beta^0 u(x), \tag{5}$$

where $u(x) = e^{-\alpha(h_0 + x\cos\theta)}$ is the ratio of density at point x to the density at earth's surface. The other scattering term we need must describe the fraction of light scattered into the viewing direction (θ,ϕ) from a solid angle ω. This is commonly denoted $\beta(\omega,\theta,\phi,h)$. Using the same trick as for $\beta(h)$, it can be rewritten as

$$\beta(\omega,\theta,\phi,h(x)) = \beta^0(\omega,\theta,\phi)u(x). \tag{6}$$

4.1 Extinction Factor

The extinction factor τ can be determined directly given our assumptions of an exponential density of particles. Attenuation of light due to particles with total scattering coefficient β over a distance s is given by $e^{-\int_0^s \beta dx}$. Using equation 5 and integrating, we have

$$\tau = e^{-\int_0^s \beta^0 u(x)dx} = e^{-\beta^0 e^{-\alpha h_0}\frac{(1-e^{-\alpha\cos\theta s})}{\alpha\cos\theta}}.$$

For convenience, we make the substitutions $K = -\frac{\beta^0}{\alpha\cos\theta}$ and $H = e^{-\alpha h_0}$, allowing the extinction factor to be neatly written as $e^{-K(H-u(s))}$ for a single type of particle.

Atmosphere contains both molecules and haze, both of which scatter light. The scattering properties of a particle is independent of the presence of other particles and therefore the total attenuation due to the presence of two types of particles is equal to the product of the attenuation by each individual particles. This means the total extinction due to both these particles is

$$\tau = e^{-K_1(H_1-u_1(s))}e^{-K_2(H_2-u_2(s))}, \tag{7}$$

where the subscript "1" denotes haze particles and the subscript "2" denotes molecular particles.

4.2 Light Scattered into Viewing Ray

At every point on the ray, light from the sun/sky is scattered into the viewing direction. Let $L^s(\omega)$ denote the spectral radiance of sun and sky in the direction ω. We can assume that the spectral radiance from sun and sky, $L^s(\omega)$ does not depend on altitude because the viewer and source are close to the earth's surface. Let $S(\theta,\phi,x)$ be the term to denote the light scattered into the viewing

direction (θ, ϕ) at point x. Using the angular scattering coefficient from equation 6, we can express the light scattered into the viewing direction at x as

$$\begin{aligned} S(\theta,\phi,x) &= \int L^s(\omega)\beta(\omega,\theta,\phi,h)d\omega \\ &= \int L^s(\omega)\beta^0(\omega,\theta,\phi)u(x)d\omega \\ &= S^0(\theta,\phi)u(x), \end{aligned}$$

where $S^0(\theta,\phi) = \int L^s(\omega)\beta^0(\omega,\theta,\phi)d\omega$ is the light scattered into the viewing direction (θ,ϕ) at ground level.

If we denote attenuation (equation 7) from 0 to x along viewing ray as $\tau(0..x)$ then, the total light scattered into the viewing direction for a single type of particle is:

$$L_{\text{in}} = \int_0^s S(\theta,\phi,x)\tau(0..x)dx = \int_0^s S^0(\theta,\phi)u(x)\tau(0..x)dx.$$

Since there are two kinds of particles (haze and molecules), the total light scattered into viewing direction is:

$$\begin{aligned} L_{\text{in}} &= \int_0^s S_1^0(\theta,\phi)u_1(x)\tau(0..x)dx + \\ &\quad \int_0^s S_2^0(\theta,\phi)u_2(x)\tau(0..x)dx \\ &= S_1^0(\theta,\phi)I_1 + S_2^0(\theta,\phi)I_2, \end{aligned} \tag{8}$$

where $I_i = \int_0^s u_i(x)\tau(0..x)dx$. A table of $S_1^0(\theta,\phi)$ and $S_2^0(\theta,\phi)$ for different θ and ϕ can be precomputed thus avoiding expensive computation for every pixel.

We show how to solve I_1 in this paper; the solution for I_2 is analogous. First we expand $\tau(0..x)$ and examine the results.

$$I_1 = \int_0^s u_1(x)e^{-K_1(H_1-u_1(x))}e^{-K_2(H_2-u_2(x))}dx. \tag{9}$$

If $|\alpha s\cos\theta| \ll 1$ which would happen when the viewing ray is close to horizon or the distances considered are small, the term $e^{-K(H-u(x))} = e^{-\beta H\frac{1-e^{-\alpha x\cos\theta}}{\alpha\cos\theta}} \approx e^{-\beta Hx}$. Thus

$$\begin{aligned} I_1 &= \int_0^s u_1(x)e^{-K_1(H_1-u_1(x))}e^{-K_2(H_2-u_2(x))}dx \\ &= \int_0^s e^{-H_1}e^{-\alpha_1 x\cos\theta}e^{-\beta_1 H_1 x}e^{-\beta_2 H_2 x}dx \\ &= e^{-H_1}\frac{1-e^{-(\alpha_1\cos\theta+\beta_1 H_1+\beta_2 H_2)s}}{\alpha_1\cos\theta+\beta_1 H_1+\beta_2 H_2}. \end{aligned} \tag{10}$$

Otherwise, two different approaches could be taken to solving these integrals. The simplest and most accurate method of calculating the integrals I_1 and I_2 are by numerical integration techniques. This is too expensive for the model to remain practical. We make approximations to the expressions above to present the results in closed form. In Equation 9 we make the following substitution, $v = u_1(x) = e^{-\alpha_1(h_0+x\cos\theta)}$. Therefore, $dv = -\alpha_1\cos\theta u_1(x)dx$. We now have

$$I_1 = -\frac{1}{\alpha_1\cos\theta}\int_{u_1(0)}^{u_1(s)} e^{-K_1(H_1-v)}e^{-K_2(H_2-u_2(x))}dv.$$

We replace the term $f(x) = e^{-K_2(H_2-u_2(x))}$ with a Hermite cubic polynomial $g(v) = av^3 + bv^2 + cv + d$ so that I_1 is integrable in closed form. The coefficients a, b, c and d for the cubic equivalent are determined such that $g(v)$ interpolates the position and slope of the endpoints of $f(x)$. The resulting integral,

$$I_1 = -\frac{1}{\alpha_1\cos\theta}\int_{u_1(0)}^{u_1(s)} e^{-K_1(H_1-v)}g(v)dv, \tag{11}$$

can be integrated by parts, leaving an analytic approximation for I_1. This result and the coefficients for the polynomial are given in the Appendix.

5 Results

Our model was implemented in a C++ path tracer [14] that accepts 30m digital elevation data. All images are of a constant albedo terrain skin of approximately 4000km^2. The 30m resolution cells visible in the foreground of the images give an idea of scale. The implementation of the model was not carefully optimized, and slowed down the program by approximately a factor of two on a MIPS R10000 processor. The images are 1000 by 750 pixels and were run with 16 samples per pixel.

Figure 7 shows the same landscape at different times of day and turbidities for a viewer looking west. Note that near sunset, there is much warm light visible in the aerial perspective for the higher turbidities. This is as expected because the high concentrations of aerosols present at high turbidities tend to forward scatter the sunlight which has had much of the blue removed by the thick atmosphere for shallow sun angles.

We used a high value for turbidity for the last picture of Figure 7. For these high values, we would typically expect an overcast sky for such high turbidities, and this is shown in the figure using the CIE overcast sky luminance and a flat spectral curve. For intermediate turbidities our model and the overcast model should be interpolated between as recommended for the CIE luminance models. These unusual conditions are the "hazy, hot, and humid" weather familiar to the inland plains.

Figure 8 shows a comparison between the model used by Ward-Larson in the *Radiance* package and our model for a summer sky a half hour before sunset with turbidity 6. Our implementation of Ward-Larson's model uses the correct luminance but the relative spectral curve of the zenith. It correctly sets the attenuation at one kilometer and uses an exponential interpolant elsewhere. For in-scattering it uses the product of the zenith spectral radiance and the complement of the attenuation factor. This is our best estimate for setting the "ambient" in-scattering term suggested by Ward-Larson. We could certainly hand-tune this in-scattering term to produce better results for one view, but it would cause problems for other views because Ward-Larson's model does not take view direction into account. Note that for our model at sunset the east view always has a blue-shift in the hue (because of backward Rayleigh scattering), and a yellowish shift for west views depending upon turbidity. This effect is not possible to achieve with a model that does not vary with direction.

6 Conclusions and Future Work

We have presented a reasonably accurate analytic model of skylight that is relatively easy to use. It captures the effects of different atmospheric conditions and times of day. In the same spirit, we have presented a model for aerial perspective. The use of both models greatly enhances the realism of outdoor rendering with minimal performance penalties, which may allow widespread use of these effects for rendering.

Our models use uniform (exponential or nearly exponential) density distributions of particles. These assumptions do not hold for cloudy (or partly cloudy) skies. They also do not hold for fog or

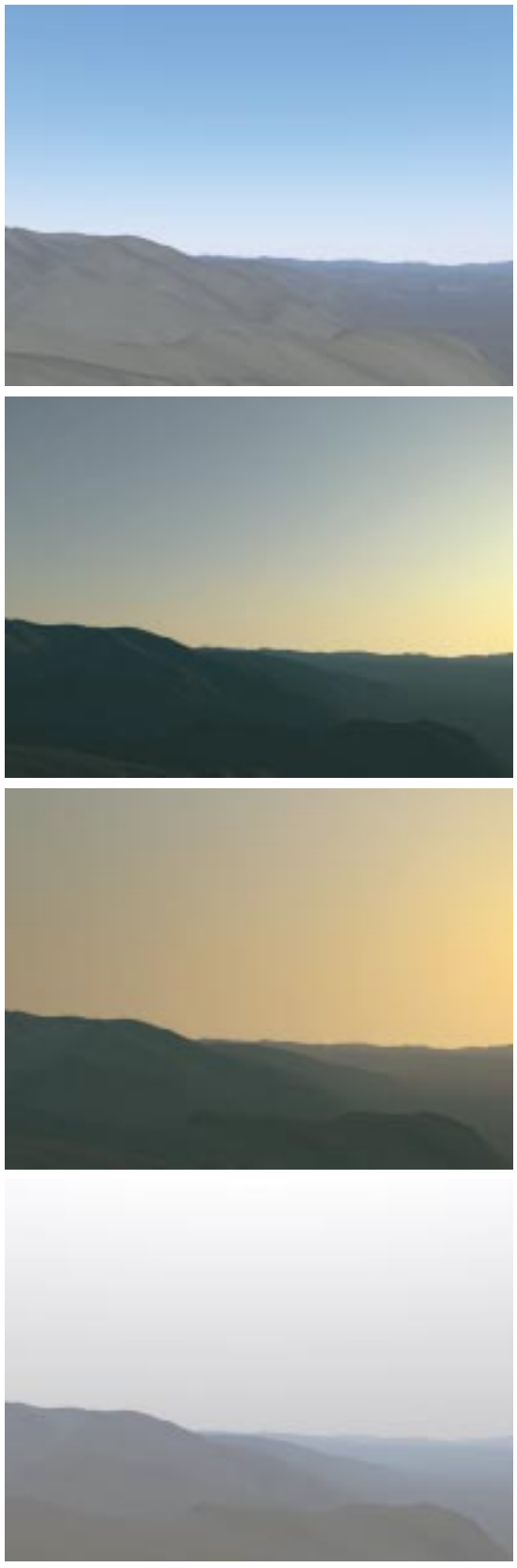

Figure 7: *The new model looking west at different times/turbidities. Top to bottom: morning, tubididity 2; evening, turbidity 2; evening, turbidity 6; overcast, turbidity 10.*

Figure 8: *Top: the CIE clear sky model using constant chromaticity coordinates and Ward-Larson's aerial perspective approximation for east viewing directions and the same viewpoint. Bottom: the new model. Note the change in hue for different parts of the sky for the new model.*

the effects of localized pollution sources and inversion effects that often occur near some large cities. In these cases the density distribution of particles is much more complicated than in our model. In these cases, our model can be used as boundary conditions for more complex simulations.

7 Acknowledgments

Thanks to Sumant Pattanaik for the original CIE sky model implementation, to Chuck Hansen and the Los Alamos ACL lab for enabling computer runs, to Bill Thompson and Simon Premoze for supplying digital terrain data, and to the Utah SGI Visual Supercomputing Center for thousands of hours of CPU time. This work was supported by NSF awards 9731859 and 9720192, and the NSF STC for Computer Graphics & Visualization.

A Appendix

Although much of the data in this appendix is available in the literature, it is not in sources readily accessible to most graphics professionals. The information here should allow users to implement our model without sources other than this paper.

A.1 Transmittance expressions for atmospheric constituents

Simple results are given describing the attenuation of direct radiation by various atmospheric constituents using the data given by Iqbal [13]. The formulas permit atmospheric parameters such as ozone layer thickness, precipitable water vapor and turbidity to be varied independently. These results are used in the computation of sunlight received at earth's surface.

Relative optical mass m is given by the following approximation, where sun angle θ_s is in radians:

$$m = \frac{1}{\cos\theta_s + 0.15 * (93.885 - \theta_s \frac{180}{\pi})^{-1.253}}.$$

Transmittance due to Rayleigh scattering of air molecules ($\tau_{r,\lambda}$), Angstrom's turbidity formula for aerosol ($\tau_{a,\lambda}$), transmittance due to ozone absorption ($\tau_{o,\lambda}$), transmittance due to mixed gases absorption ($\tau_{g,\lambda}$) and transmittance due to water vapor absorption ($\tau_{wa,\lambda}$) are given by:

$$\begin{aligned}
\tau_{r,\lambda} &= e^{-0.008735\lambda^{-4.08}m}, \\
\tau_{a,\lambda} &= e^{-\beta\lambda^{-\alpha}m}, \\
\tau_{o,\lambda} &= e^{-k_{o,\lambda}lm}, \\
\tau_{g,\lambda} &= e^{-1.41k_{g,\lambda}m/(1+118.93k_{g,\lambda}m)^{0.45}}, \\
\tau_{wa,\lambda} &= e^{-0.2385k_{wa,\lambda}wm/(1+20.07k_{wa,\lambda}wm)^{0.45}},
\end{aligned}$$

where β is Angstrom's turbidity coefficient, α is the wavelength exponent, $k_{o,\lambda}$ is the attenuation coefficient for ozone absorption, l is the amount of ozone in *m* at NTP, $k_{g,\lambda}$ is the attenuation coefficient of mixed gases absorption, $k_{wa,\lambda}$ is the attenuation coefficient of water vapor absorption, w is the precipitable water vapor in *m* and λ is the wavelength in μm. The coefficient β varies with turbidity T and is approximately given by $0.04608T - 0.04586$. As originally suggested by Angstrom, we use $\alpha = 1.3$. A value of 0.0035m for l and 0.02m for w is commonly used.

The spectrums $k_{o,\lambda}$, $k_{g,\lambda}$ and $k_{wa,\lambda}$ are found in Table 2.

A.2 Skylight Distribution Coefficients and Zenith Values

The distribution coefficients vary with turbidity and the zenith values are functions of turbidity and sun position.

The coefficients for the Y, x and y distribution functions are:

$$\begin{bmatrix} A_Y \\ B_Y \\ C_Y \\ D_Y \\ E_Y \end{bmatrix} = \begin{bmatrix} 0.1787 & -1.4630 \\ -0.3554 & 0.4275 \\ -0.0227 & 5.3251 \\ 0.1206 & -2.5771 \\ -0.0670 & 0.3703 \end{bmatrix} \begin{bmatrix} T \\ 1 \end{bmatrix}$$

$$\begin{bmatrix} A_x \\ B_x \\ C_x \\ D_x \\ E_x \end{bmatrix} = \begin{bmatrix} -0.0193 & -0.2592 \\ -0.0665 & 0.0008 \\ -0.0004 & 0.2125 \\ -0.0641 & -0.8989 \\ -0.0033 & 0.0452 \end{bmatrix} \begin{bmatrix} T \\ 1 \end{bmatrix}$$

$$\begin{bmatrix} A_y \\ B_y \\ C_y \\ D_y \\ E_y \end{bmatrix} = \begin{bmatrix} -0.0167 & -0.2608 \\ -0.0950 & 0.0092 \\ -0.0079 & 0.2102 \\ -0.0441 & -1.6537 \\ -0.0109 & 0.0529 \end{bmatrix} \begin{bmatrix} T \\ 1 \end{bmatrix}$$

Absolute value of zenith luminance in K cd m^{-2}:

$$Y_z = (4.0453T - 4.9710)\tan\chi - 0.2155T + 2.4192,$$

$\theta\backslash\lambda$	400	450	550	650	850
1	4.192	4.193	4.177	4.147	4.072
4	3.311	3.319	3.329	3.335	3.339
7	2.860	2.868	2.878	2.883	2.888
10	2.518	2.527	2.536	2.542	2.547
30	1.122	1.129	1.138	1.142	1.147
60	0.3324	0.3373	0.3433	0.3467	0.3502
80	0.1644	0.1682	0.1730	0.1757	0.1785
90	0.1239	0.1275	0.1320	0.1346	0.1373
110	0.08734	0.09111	0.09591	0.09871	0.10167
120	0.08242	0.08652	0.09179	0.09488	0.09816
130	0.08313	0.08767	0.09352	0.09697	0.10065
150	0.09701	0.1024	0.1095	0.1137	0.1182
180	0.1307	0.1368	0.1447	0.1495	0.1566

Table 1: Scattering term $\eta(\theta)$ for Mie scattering.

where $\chi = (\frac{4}{9} - \frac{T}{120})(\pi - 2\theta_s)$.

Zenith chromaticity (x_z, y_z):

$$x_z = \begin{bmatrix} T^2 & T & 1 \end{bmatrix} \begin{bmatrix} 0.0017 & -0.0037 & 0.0021 & 0.000 \\ -0.0290 & 0.0638 & -0.0320 & 0.0039 \\ 0.1169 & -0.2120 & 0.0605 & 0.2589 \end{bmatrix} \begin{bmatrix} \theta_s^3 \\ \theta_s^2 \\ \theta_s \\ 1 \end{bmatrix}$$

$$y_z = \begin{bmatrix} T^2 & T & 1 \end{bmatrix} \begin{bmatrix} 0.0028 & -0.0061 & 0.0032 & 0.000 \\ -0.0421 & 0.0897 & -0.0415 & 0.0052 \\ 0.1535 & -0.2676 & 0.0667 & 0.2669 \end{bmatrix} \begin{bmatrix} \theta_s^3 \\ \theta_s^2 \\ \theta_s \\ 1 \end{bmatrix}$$

A.3 Scattering Coefficients

In scattering theory, the angular scattering coefficient and the total scattering coefficient determine how the light is scattered by particles. For our work Rayleigh scattering is used for gas molecules and Mie scattering theory is used for haze particles. Here we give the scattering coefficients for gas molecules and haze. Notice that the total scattering coefficient is the integral of angular scattering coefficient in all directions, for example $\beta = \int \beta(\theta) dw$. For an elaborate discussion on scattering, see [21, 28].

The angular and total scattering coefficients for Rayleigh scattering for molecules are:

$$\begin{aligned}
\beta_m(\theta) &= \frac{\pi^2(n^2-1)^2}{2N\lambda^4}(\frac{6+3p_n}{6-7p_n})(1+\cos^2\theta), \\
\beta_m &= \frac{8\pi^3(n^2-1)^2}{3N\lambda^4}(\frac{6+3p_n}{6-7p_n}),
\end{aligned}$$

where n is refractive index of air and is 1.0003 in the visible spectrum, N is number of molecules per unit volume and is $2.545\text{x}10^{25}$ for air at 228.15K and 1013mb, p_n is the depolarization factor and 0.035 is considered standard for air.

The angular and total scattering coefficients for Mie scattering for haze are:

$$\begin{aligned}
\beta_p(\theta) &= 0.434c(\frac{2\pi}{\lambda})^{v-2}\frac{1}{2}\eta(\theta), \\
\beta_p &= 0.434c\pi(\frac{2\pi}{\lambda})^{v-2}K,
\end{aligned}$$

where c is the concentration factor that varies with turbidity T and is $(0.6544T - 0.6510)\text{x}10^{-16}$ and v is Junge's exponent with a value of 4 for the sky model. A table for $\eta(\theta, \lambda)$ for $v = 4$ (Source: [3]) is given in Table 1, and the spectrum for K is given in Table 2.

A.4 Aerial Perspective Formulas

The expression for aerial perspective is $L(s) = L_0\tau + L_{\text{in}}$, where L_0 is the spectral radiance of the distant object. The extinction factor τ is given by equation 7. The light scattered into the ray is handled differently depending upon the viewing angle θ and distance s. For $|\alpha s \cos\theta| \ll 1$ we use equations 10 and 8. Otherwise we need to integrate the expression from equation 11. First the integration:

$$\begin{aligned} I_1 &= -\frac{1}{\alpha_1 \cos\theta}\int_{u_1(0)}^{u_1(s)} e^{-K_1(H_1-v)} g(v)\,dv \\ &= -\frac{1}{\alpha_1 \cos\theta}[e^{-K_1(H_1-v)}(\frac{g(v)}{K_1} - \frac{g'(v)}{K_1^2} + \frac{g''(v)}{K_1^3} - \frac{g'''(v)}{K_1^4})]_{H_1}^{u_1(s)} \\ &= -\frac{1}{\alpha_1 \cos\theta}((e^{-K_1(H_1-u_1(s))}) \times \\ &\quad (\frac{g(u_1(s))}{K_1} - \frac{g'(u_1(s))}{K_1^2} + \frac{g''(u_1(s))}{K_1^3} - \frac{g'''(u_1(s))}{K_1^4}) - \\ &\quad (\frac{g(H_1)}{K_1} - \frac{g'(H_1)}{K_1^2} + \frac{g''(H_1)}{K_1^3} - \frac{g'''(H_1)}{K_1^4})) \end{aligned}$$

The values of a, b, c, and d for the function $g(v) = av^3 + bv^2 + cv + d$ to approximate $f(x) = e^{-K_2(H_2-u_2(x))}$ where $v = u_1(x)$ are determined by the solution to the following system of linear equations:

$$\begin{bmatrix} H_1^3 & H_1^2 & H_1 & 1 \\ u_1(s)^3 & u_1(s)^2 & u_1(s) & 1 \\ 3H_1^2 & 2H_1 & 1 & 0 \\ 3u_1(s)^2 & 2u_1(s) & 1 & 0 \end{bmatrix} \begin{bmatrix} a \\ b \\ c \\ d \end{bmatrix} = \begin{bmatrix} 1 \\ f(s) \\ f'(0) \\ f'(s) \end{bmatrix}$$

The values for the exponential decay constant α are: $\alpha_{haze} = 0.8333\ \text{km}^{-1}$ and $\alpha_{molecules} = 0.1136\ \text{km}^{-1}$.

A.5 Converting Tristimulous Values to Spectral Radiance

From Wyszecki and Stiles [32], the relative spectral radiant power $S_D(\lambda)$ of a D-illuminant is given by a linear combination of mean spectral radiant power $S_0(\lambda)$ and first two eigen vector functions $S_1(\lambda)$ and $S_2(\lambda)$ used in calculating daylight illuminants. $S_D(\lambda) = S_0(\lambda) + M_1 S_1(\lambda) + M_2 S_2(\lambda)$. Scalar multiples M_1 and M_2 are functions of chromaticity values x and y and are given by

$$\begin{aligned} M_1 &= \frac{-1.3515 - 1.7703x + 5.9114y}{0.0241 + 0.2562x - 0.7341y}, \\ M_2 &= \frac{0.0300 - 31.4424x + 30.0717y}{0.0241 + 0.2562x - 0.7341y}. \end{aligned}$$

A.6 Sun Position

Sun position is given by angle from zenith (θ_s) and azimuth angle (ϕ_s) and they depend on the time of the day, date, latitude and longitude (see Figure 4). Solar time can be calculated from the standard time by using the formula

$$t = t_s + 0.170\sin(\frac{4\pi(J-80)}{373}) - 0.129\sin(\frac{2\pi(J-8)}{355}) + \frac{12(SM-L)}{\pi},$$

where t is solar time in decimal hours, t_s is standard time in decimal hours, SM is standard meridian for the time zone in radians, L is site longitude in radians and J is Julian date (the day of the year as an integer in the range 1 to 365).

The solar declination (δ) in radians is approximated by

$$\delta = 0.4093\sin(\frac{2\pi(J-81)}{368}).$$

λ (nm)	K	S_0	S_1	S_2	Sun rad.	k_o	k_{wa}	k_g
380	0.650	63.4	38.5	3	16559	-	-	-
390	0.653	65.8	35	1.2	16233.7	-	-	-
400	0.656	94.8	43.4	-1.1	21127.5	-	-	-
410	0.658	104.8	46.3	-0.5	25888.2	-	-	-
420	0.661	105.9	43.9	-0.7	25829.1	-	-	-
430	0.662	96.8	37.1	-1.2	24232.3	-	-	-
440	0.663	113.9	36.7	-2.6	26760.5	-	-	-
450	0.666	125.6	35.9	-2.9	29658.3	0.3	-	-
460	0.667	125.5	32.6	-2.8	30545.4	0.6	-	-
470	0.669	121.3	27.9	-2.6	30057.5	0.9	-	-
480	0.670	121.3	24.3	-2.6	30663.7	1.4	-	-
490	0.671	113.5	20.1	-1.8	28830.4	2.1	-	-
500	0.672	113.1	16.2	-1.5	28712.1	3	-	-
510	0.673	110.8	13.2	-1.3	27825	4	-	-
520	0.674	106.5	8.6	-1.2	27100.6	4.8	-	-
530	0.676	108.8	6.1	-1	27233.6	6.3	-	-
540	0.677	105.3	4.2	-0.5	26361.3	7.5	-	-
550	0.678	104.4	1.9	-0.3	25503.8	8.5	-	-
560	0.679	100	0	0	25060.2	10.3	-	-
570	0.679	96	-1.6	0.2	25311.6	12	-	-
580	0.680	95.1	-3.5	0.5	25355.9	12	-	-
590	0.681	89.1	-3.5	2.1	25134.2	11.5	-	-
600	0.682	90.5	-5.8	3.2	24631.5	12.5	-	-
610	0.682	90.3	-7.2	4.1	24173.2	12	-	-
620	0.683	88.4	-8.6	4.7	23685.3	10.5	-	-
630	0.684	84	-9.5	5.1	23212.1	9	-	-
640	0.684	85.1	-10.9	6.7	22827.7	7.9	-	-
650	0.685	81.9	-10.7	7.3	22339.8	6.7	-	-
660	0.685	82.6	-12	8.6	21970.2	5.7	-	-
670	0.685	84.9	-14	9.8	21526.7	4.8	-	-
680	0.686	81.3	-13.6	10.2	21097.9	3.6	-	-
690	0.686	71.9	-12	8.3	20728.3	2.8	1.6	-
700	0.687	74.3	-13.3	9.6	20240.4	2.3	2.4	-
710	0.687	76.4	-12.9	8.5	19870.8	1.8	1.25	-
720	0.688	63.3	-10.6	7	19427.2	1.4	100	-
730	0.688	71.7	-11.6	7.6	19072.4	1.1	87	-
740	0.689	77	-12.2	8	18628.9	1	6.1	-
750	0.689	65.2	-10.2	6.7	18259.2	0.9	0.1	-
760	0.689	47.7	-7.8	5.2	-	0.7	1e-03	3.0
770	0.689	68.6	-11.2	7.4	-	0.4	1e-03	0.21
780	0.689	65	-10.4	6.8	-	-	0.06	-

Table 2: Spectral quantities used in the model (SI units).

Solar position (θ_s, ϕ_s) can be computed from the solar declination angle, latitude and longitude.

$$\begin{aligned} \theta_s &= \frac{\pi}{2} - \arcsin(\sin l \sin\delta - \cos l \cos\delta \cos\frac{\pi t}{12}), \\ \phi_s &= \arctan(\frac{-\cos\delta \sin\frac{\pi t}{12}}{\cos l \sin\delta - \sin l \cos\delta \cos\frac{\pi t}{12}}), \end{aligned}$$

where θ_s is solar angle from zenith in radians, ϕ_s is solar azimuth in radians, l is site latitude in radians, δ is solar declination in radians and t is solar time in decimal hours. Solar angles from zenith are between 0 and $\pi/2$ and angles above $\pi/2$ indicate sun below horizon. Positive solar azimuthal angles represent direction west of south.

A.7 Spectra

There are several spectral quantities used in the model: K for $v = 4$ used in the calculation of Mie scattering coefficient; S_0, S_1, S_2 spectrums [32]; the sun's spectral radiance in $\text{Wm}^{-2}\text{nm}^{-1}\text{sr}^{-1}$. The latter was calculated from the spectral distribution of solar radiation incident at top of the atmosphere as adopted by NASA as a standard for use in engineering design [5]. These quantities can be found in Table 2. The spectral curves k_o in m^{-1}, k_{wa} in m^{-1} and k_g used in the sunlight computation are also listed (Source: [13]).

References

[1] BLINN, J. F. Light reflection functions for simulation of clouds and dusty surfaces. vol. 16, pp. 21–29.

[2] BRUNGER, A. P., AND HOOPER, F. C. Anisotropic sky radiance model based on narrow field of view measurements of shortwave radiance. *Solar Energy* (1993).

[3] BULLRICH, K. Scattered radiation in the atmosphere. In *Advances in Geophysics*, vol. 10. 1964.

[4] CIE-110-1994. Spatial distribution of daylight - luminance distributions of various reference skies. Tech. rep., International Commission on Illumination, 1994.

[5] COULSON, K. L. *Solar and Terrestrial Radiation*. Academic Press, 1975.

[6] DA VINCI, L. *The Notebooks of Leonardo da Vinci*, vol. 1. Dover, 1970.

[7] DOBASHI, Y., NISHITA, T., KANEDA, K., AND YAMASHITA, H. Fast display method of sky color using basis functions. In *Pacific Graphics '95* (Aug. 1995).

[8] EBERT, D., MUSGRAVE, K., PEACHEY, D., PERLIN, K., AND WORLEY. *Texturing and Modeling: A Procedural Approach*, second ed. Academic Press, 1998.

[9] ELTERMAN, L. Aerosol measurements in the troposphere and stratosphere. *Applied Optics 5*, 11 (November 1966), 1769–1776.

[10] GOLDSTEIN, E. B. *Sensation and Perception.* Wadsworth, 1980.

[11] GRACE, A. *Optimization Toolbox for use with MATLAB: User's Guide*. The Math Works Inc., 1992.

[12] INEICHEN, P., MOLINEAUX, B., AND PEREZ, R. Sky luminance data validation: comparison of seven models with four data banks. *Solar Energy 52*, 4 (1994), 337–346.

[13] IQBAL, M. *An Introduction to Solar Radiation.* Academic Press, 1983.

[14] KAJIYA, J. T. The rendering equation. In *Computer Graphics (SIGGRAPH '86 Proceedings)* (Aug. 1986), D. C. Evans and R. J. Athay, Eds., vol. 20, pp. 143–150.

[15] KANEDA, K., OKAMOTO, T., NAKAME, E., AND NISHITA, T. Photorealistic image synthesis for outdoor scenery under various atmospheric conditions. *The Visual Computer 7*, 5 and 6 (1991), 247–258.

[16] KARAYEL, M., NAVVAB, M., NE'EMAN, E., AND SELKOWITZ, S. Zenith luminance and sky luminance distributions for daylighting calculations. *Energy and Buildings 6*, 3 (1984), 283–291.

[17] KAUFMAN, J. E., Ed. *The Illumination Engineering Society Lighting Handbook, Reference Volume*. Waverly Press, Baltimore, MD, 1984.

[18] KLASSEN, R. V. Modeling the effect of the atmosphere on light. *ACM Transactions on Graphics 6*, 3 (1987), 215–237.

[19] LYNCH, D. K., AND LIVINGSTON, W. *Color and Light in Nature*. Cambridge University Press, 1995.

[20] MAX, N. L. Atmospheric illumination and shadows. In *Computer Graphics (SIGGRAPH '86 Proceedings)* (Aug. 1986), vol. 20, pp. 117–24.

[21] MCCARTNEY, E. J. *Optics of the Atmosphere*. Wiley publication, 1976.

[22] MINNAERT, M. *Light and Color in the Open Air*. Dover, 1954.

[23] NAKAMAE, E., KANEDA, K., OKAMOTO, T., AND NISHITA, T. A lighting model aiming at drive simulators. In *Computer Graphics (SIGGRAPH '90 Proceedings)* (Aug. 1990), F. Baskett, Ed., vol. 24, pp. 395–404.

[24] NIMEROFF, J., DORSEY, J., AND RUSHMEIER, H. Implementation and analysis of an image-based global illumination framework for animated environments. *IEEE Transactions on Visualization and Computer Graphics 2*, 4 (Dec. 1996). ISSN 1077-2626.

[25] NISHITA, T., DOBASHI, Y., KANEDA, K., AND YAMASHITA, H. Display method of the sky color taking into account multiple scattering. In *Pacific Graphics '96* (1996), pp. 117–132.

[26] NISHITA, T., SIRAI, T., TADAMURA, K., AND NAKAMAE, E. Display of the earth taking into account atmospheric scattering. In *Computer Graphics (SIGGRAPH '93 Proceedings)* (Aug. 1993), J. T. Kajiya, Ed., vol. 27, pp. 175–182.

[27] R. PEREZ, R. SEALS, J. M., AND INEICHEN, P. An all-weather model for sky luminance distribution. *Solar Energy* (1993).

[28] RAYLEIGH, L. On the scattering of light by small particles. *Philosophical Magazine 41* (1871), 447–454.

[29] TAKAGI, A., TAKAOKA, H., OSHIMA, T., AND OGATA, Y. Accurate rendering technique based on colorimetric conception. In *Computer Graphics (SIGGRAPH '90 Proceedings)* (Aug. 1990), F. Baskett, Ed., vol. 24, pp. 263–272.

[30] WARD, G. J. The RADIANCE lighting simulation and rendering system. In *Proceedings of SIGGRAPH '94 (Orlando, Florida, July 24–29, 1994)* (July 1994), A. Glassner, Ed., Computer Graphics Proceedings, Annual Conference Series, ACM SIGGRAPH, ACM Press, pp. 459–472. ISBN 0-89791-667-0.

[31] WARD-LARSON, G. Personal Communication, 1998.

[32] WYSZECKI, G., AND W.S.STILES. *Color Science*. Wiley-Interscience publication, 1982.

[33] YU, Y., AND MALIK, J. Recovering photometric properties of architectural scenes from photographs. In *SIGGRAPH 98 Conference Proceedings* (July 1998), M. Cohen, Ed., Annual Conference Series, ACM SIGGRAPH, Addison Wesley, pp. 207–218. ISBN 0-89791-999-8.